Formation and Characterization of New Magnesium Aluminum Hydroxycarbonates

IAN E. GREY* AND ROLAND RAGOZZINI†

CSIRO, Division of Mineral Products, P.O. Box 124, Port Melbourne, Victoria 3207, Australia

The removal of aluminum from strong caustic soda solutions (simulated paper pulp liquors) was studied using the addition of calcined magnesite to precipitate magnesium aluminum hydroxycarbonate phases. For aluminum concentrations higher than about 150 ppm the precipitated phase was hydrotalcite, whereas for lower aluminum concentrations, new hydroxycarbonate phases formed. For solution temperatures above 70°C the phase which formed was characterized as a 1:1 unit cell intergrowth of brucite and hydrotalcite. The new phase is isostructural with coalingite, having a rhombohedral unit cell, $R\bar{3}m$, $a = 3.108(4)$ Å, $c = 38.3(1)$ Å, and a composition of $[Mg_{0.88}Al_{0.12}(OH)_2]_2 \cdot [(CO_3)_{0.12}(H_2O)_{0.64}]$. With variation of solution temperature and concentration, other phases responsible for aluminum removal were formed and identified, including higher order brucite–hydrotalcite intergrowths and aluminum-containing brucite. © 1991 Academic Press, Inc.

1. Introduction

In paper pulp production by the soda-anthraquinone process (*1*), the lignin content of the wood is leached in concentrated caustic soda solution. The spent solution, termed black liquor, is regenerated by a variety of processes to give a "white liquor" which is returned to the wood digestion plant. Non-process elements such as aluminum, derived, for example, from residual soil adhering to the wood, accumulate in the caustic solution and can lead to scale formation if not removed (*2*). An effective removal method is the addition of reactive magnesium compounds to precipitate aluminum as hydrotalcite (*3*). This phase is a mixed metal hydroxide conforming to the general formula $[(M^{II})_{1-x}(M^{III})_x(OH)_2]^{x+}$ $(Y^{z-})_{x/z} \cdot nH_2O$, where $M^{II} = Mg$, $M^{III} = Al$, and $Y = CO_3^{2-}$. Carbonate ions are always found to some extent in caustic solutions.

In a study of the removal of low levels (ca. 100 ppm) of aluminum from simulated white liquors using calcined magnesium carbonates, we found that the main phase responsible for aluminum removal was *not* hydrotalcite but a new mixed metal hydroxycarbonate. This was shown to be a 1:1 atomic scale intergrowth between hydrotalcite and brucite ($Mg(OH)_2$) type structures. Variation of experimental conditions led to the formation of higher order intergrowths and Al-substituted brucite. We describe here the results of characterization studies on the new intergrowth phases.

---

* To whom correspondence should be addressed.
† Present address: Albright and Wilson (Australia) Ltd., Yarraville, Victoria 3013, Australia.

2. Previous Studies on Mg–Al Hydroxycarbonates

Magnesium aluminum hydroxycarbonates have long been known as the minerals hydrotalcite and manasseite (4, 5). Their structures (6, 7) consist of positively charged brucite type layers, $[Mg_{1-x}Al_x(OH)_2]^{x+}$, separated by layers containing carbonate ions and water molecules. Hydrotalcite and manasseite are dimorphic forms having the same composition but differing in the stacking sequence of brucite hydroxyl layers. In hydrotalcite the sequence is AB . . . BC . . . CA . . . AB, giving a rhombohedral cell with $a \sim 3$ Å, $c \sim 23.4$ Å (3×7.8 Å), whereas in manasseite the sequence is AB . . . BA . . . AB, giving a hexagonal cell with $c \sim 15.6$ Å (2×7.8 Å).

Numerous papers have described the synthesis of Mg, Al hydrotalcite-like phases by coprecipitation from chloride solution using NaOH (8–12). Displacement of interlayer Cl^- by CO_3^{2-} to form the hydroxycarbonates was effected by addition of Na_2CO_3 (11, 12) or by dialysis (9, 10). The formation of hydroxycarbonates from solid starting phases was demonstrated by Besson and co-workers (13, 14) using mixtures of $Mg(OH)_2$ or $MgCO_3$ and $Al(OH)_3$ in Na_2CO_3 solutions. They also carried out experiments in which the solid phases were separated in dialysis sacks, and obtained hydrotalcite formation in the dialysis medium (pH ~9), leading them to propose the solution reaction: $Al(OH)_4^- + 2MgOH^+ = [AlMg_2(OH)_6]^+$.

The composition range for single-phase synthetic hydroxycarbonates is generally reported to be $0.2 < x < 0.33$ (12, 15), although a recent study using hydrothermal syntheses extended the upper composition range to $x = 0.44$ (16). For $x < 0.2$, X-ray diffraction (XRD) studies showed a two-phase mixture of hydrotalcite plus brucite (or plus hydromagnesite for hydrothermally treated samples (12)). The extent of aluminum incorporation into brucite was studied by Mascolo and co-workers (17) using hydrothermal treatment of mixtures of alumina gel and MgO. The incorporation was very low, $[Al]/[Al + Mg] = 0.02$ at 50°C, and 0.05 at 160°C.

3. Experimental

Simulated white liquors were made by dissolving weighed amounts of AR grade NaOH and Na_2CO_3 in distilled water, then adding aluminum in the form of high purity thin foil. In accordance with plant practice, the two parameters used to characterize the white liquor are causticity and soda strength. Causticity is the atomic percentage of sodium that is present as hydroxide, i.e., $[Na]_{in\ NaOH}/[Na]_{total} \times 100$, and soda strength is the total sodium content, expressed here as g liter^{-1} of NaOH.

The MgO additive was obtained by calcination of synthetic hydromagnesite, $Mg_5(CO_3)_4(OH)_2 \cdot 4H_2O$, from Tokuyama Soda Co. (18) and BDH laboratory grade magnesite. MgO obtained by calcining BDH laboratory grade basic magnesium carbonate at 1100°C for 2 hr was supplied by Associated Pulp and Paper Mills. The calcinations were carried out in air in an electric muffle furnace. Small quantities (1–5 g) of the magnesites were heated in platinum dishes for 1 hr at the desired temperature and then cooled and stored in a vacuum dessicator.

For the aluminum removal experiments, labeled AR-1 to 308, 100 ml of simulated white liquor was measured into a polymethylpentene screw-cap bottle and preheated to a set temperature in a Julabo shaking water bath. A weighed mass of MgO corresponding to a [Mg]/[Al] atomic ratio of 10.5 was added to the solution and the shaking mechanism started. After agitation for a predetermined time the solution was filtered without cooling using a Milli-

pore alkali-resistant 0.6-μm membrane filter, type HVLP-047. The precipitate was repeatedly washed with distilled water, dried at 60°C, and weighed. The solutions and precipitate were analyzed for aluminum by AAS using a Hitachi Model Z-8000 AAS equipped with a graphite furnace for vaporization of Al_2O_3. Selected samples were analyzed for magnesium, aluminum, and sodium by ICP-AAS.

Powder XRD patterns for phases in the precipitates were obtained using a Philips diffractometer equipped with a graphite monochromator and employing Cu$K\alpha$ radiation. Residual unreacted MgO was used as an internal standard for lattice parameter refinements. Electron diffraction patterns were obtained using a Philips 400X transmission electron microscope (TEM) equipped with a Kevex X-ray detector for energy-dispersive X-ray analysis. For these studies, the precipitates were dispersed in acetone and collected on holey carbon copper grids.

Thermogravimetric (TGA) and differential thermal analyses (DTA) were performed using a Stanton Redcroft STA-780 simultaneous thermal analyzer. Sample weights of 20–30 mg were used with alumina as reference material. Runs were carried out in a static air atmosphere at a heating rate of 10° min^{-1}. Infrared spectra were recorded using a Beckman IR-33 spectrophotometer. The samples were prepared as mulls in fluorinated hydrocarbon and as KBr discs.

4. Characterization of the 1:1 Intergrowth Phase

Preliminary aluminum removal runs were carried out using white liquors having a soda strength of 260 g liter^{-1}, 95% causticity, and 100 ppm aluminum. An XRD examination of precipitates from these runs revealed the unexpected result that no hydrotalcite was formed as found by pre-

vious workers (19), even though about half of the aluminum was removed from solution. Instead, the XRD patterns exhibited peaks due to a new phase, as shown in Fig. 1a. The new phase is distinguished by three low-angle peaks with d-spacings of ~12.9, 6.4, and 4.3 Å. Characterization of this phase proved difficult because we were unable to prepare it in a pure form for analysis; residual MgO and Mg(OH)$_2$ were always present as accessory phases, as seen for the preparation AR-26 in Fig. 1a. However, by a combination of diffraction studies, thermal analyses, and infrared spectroscopy, enough information was obtained to characterize the new phase as presented below.

4.1. Diffraction Studies

TEM/EDS studies showed that the new phase contained minor aluminum and consisted of very small (<0.1 μm) thin flakes that gave diffraction patterns similar to those for brucite and hydrotalcite ($hk0$) patterns, i.e., displaying hexagonal (or trigonal) symmetry with a ~3.1 Å. This indicated a related layer structure and suggested that the observed low-angle XRD peaks were basal plane reflections (00l with $l = n$, $2n$, and $3n$. For comparison, the first (00l) reflection for Mg-rich hydrotalcite has a d-spacing of 7.92 Å (10) and that for brucite occurs at $d = 4.77$ Å. The sum of these two d-spacings is close to that for the first basal reflection of the new phase, suggesting that it is an atomic-scale 1:1 intergrowth of brucite and hydrotalcite.

The powder pattern for the new phase could be indexed on the basis of a rhombohedral cell with hexagonal parameters $a = 3.108(4)$ Å, $c = 38.3(1)$ Å (= 3 × 12.77 Å), analogous to 3R hydrotalcite. The indexed powder pattern is given in Table I. The refined peak positions showed both positive and negative departures from the measured positions, indicative of stacking faults in the layer sequence. From peak width mea-
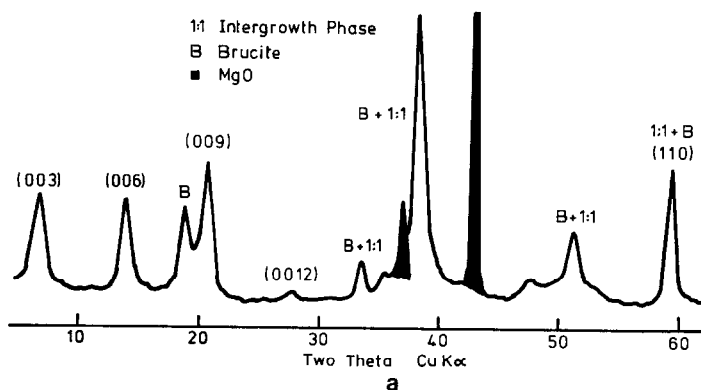
FIG. 1a. Powder X-ray diffractogram for sample AR-26, containing the 1:1 intergrowth phase, together with minor brucite and unreacted MgO.

surements the correlation length perpendicular to the layers was determined to be of the order of only 100 Å. The powder pattern intensities were calculated for the 1:1 intergrowth model, using ideal coordinates derived from the two contributing structure types and with magnesium in the $M(OH)_2$ layers. The calculated intensities, presented in Fig. 1b, show good qualitative agreement with the observed powder pattern, Fig. 1a. A schematic representation of the intergrowth structure is compared with those for brucite and hydrotalcite in Fig. 2.

A 1:1 intergrowth model requires that CO_3^{2-} and H_2O occupy the interlayer region between every second pair of $M(OH)_2$ layers, in contrast to hydrotalcite where insertion of anions expands the separation between every pair of $M(OH)_2$ layers. The lower density of interlayer anions signifies a lower level of substitution of Al for Mg in the $M(OH)_2$ layers of the intergrowth phase. We were able to confirm this quantitatively using the linear correlation between the lattice parameter a and the [Al]/[Al + Mg] atomic ratio in the $M(OH)_2$
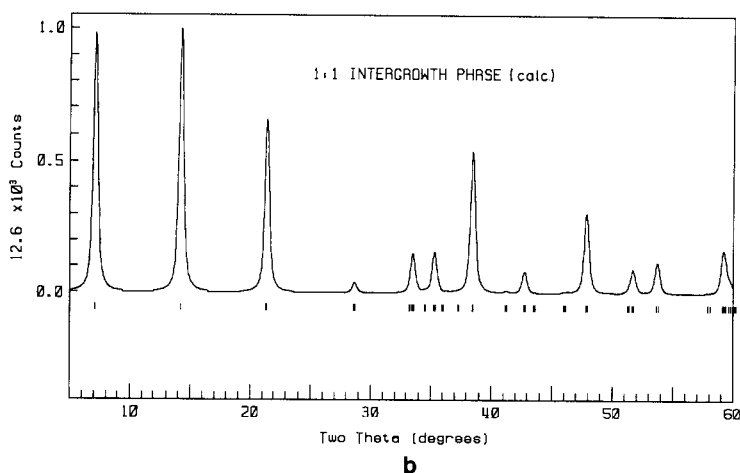
FIG. 1b. Calculated pattern for the 1:1 intergrowth phase.

layers, established by Miyata (*12*) for hydrotalcite phases. The linear relationship can be extrapolated to [Al]/[Al + Mg] = 0 by including a for $Mg(OH)_2$ (*16*). The a value of 3.108 Å for the intergrowth phase corresponds to [Al]/[Al + Mg] = 0.12. This value is halfway between that for hydrotalcite, 0.25, and that for brucite, 0. On the basis of one oxygen atom per interlayer sheet (*12*) the composition of the 1:1 intergrowth phase can then be given as

$$[Mg_{0.88}Al_{0.12}(OH)_2]_2[(CO_3)_{0.12}(H_2O)_{0.64}].$$
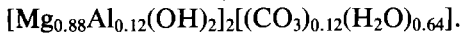
The XRD data can also be used to estimate the layer separation in the hydrotalcite part of the intergrowth phase by using the linear relationship between [Al]/[Al + Mg] and c' (c' = subcell c parameter) derived by Brindley and Kikkawa (*20*). Extrapolation of their line to [Al]/[Al + Mg] = 0.12 gives c' = 8.21 Å, which represents a considerable expansion relative to the range of c' values reported for hydrotalcites, 7.6–7.9 Å (*16*). At the same time the layer separation in the brucite part of the intergrowth phase undergoes a contraction relative to pure $Mg(OH)_2$ due to aluminum incorporation. Its value is 12.77 − 8.21 = 4.56 Å which is in reasonable agreement

FIG. 2. Schematic representations of the structures of (a) brucite, (b) hydrotalcite, and (c) the 1:1 intergrowth phase.

with a value of 4.51 Å obtained by linear extrapolation of the c vs [Al]/[Al + Mg] curve for aluminum-substituted brucite reported by Mascolo and co-workers (*17*).

Mascolo and Marino (*21*) have suggested that unit cell parameters for hydrotalcites prepared from NaOH solutions may be affected by sodium incorporation into the octahedral layers. Analyses of our solid products gave Na_2O values in the range 0.3 to 1.2 wt%, comparable to the values obtained by Mascolo and Marino (*21*). However, the sodium contents in our samples showed no systematic relationship with the compositions of the mixed-metal hydroxycarbonates. The sodium ion is too large to substitute for magnesium in the brucite layers, and the residual sodium is most likely due to incomplete washing of the strong caustic soda solution from the product.

4.2. Thermal Analyses

DTA curves are compared in Fig. 3 for three aluminum removal runs, AR-4, -24, and -26, for which the dominant product

TABLE I

X-RAY POWDER DATA FOR THE 1:1
INTERGROWTH PHASE

h k l	I_{rel}	d(obs)	d(cal)
0 0 3	30	13.0	12.8
0 0 6	30	6.39	6.39
0 0 9	46	4.30	4.26
0 0 12	2	3.21	3.19
0 1 2	12	2.67	2.66
0 1 5	6 br	2.53	2.54
0 1 8	100	2.35	2.35
0 1 14	5 br	1.903	1.919
1 0 16	23	1.784	1.789
0 1 17	6 br	1.731	1.738
1 1 0	45	1.557	1.554
1 1 6	5	1.510	1.510
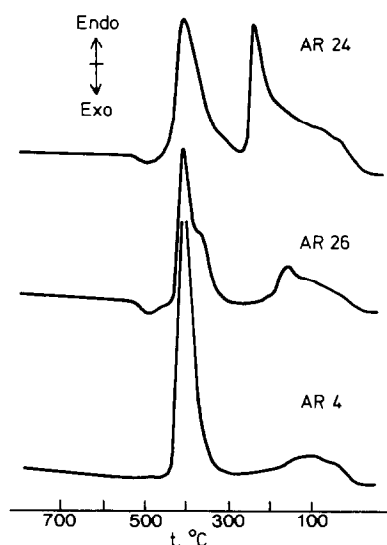
FIG. 3. DTA curves for samples AR-4, AR-24, and AR-26, containing predominantly brucite, hydrotalcite, and the 1 : 1 intergrowth phase, respectively.

was brucite, hydrotalcite, and the 1 : 1 intergrowth phase, respectively. The DTA peak positions and TGA weight losses are reported in Table II. The $Mg(OH)_2$ sample (bottom curve) shows a sharp endotherm due to dehydroxylation at 408°C, together with a weak broad endotherm due to loss of adsorbed water. The dehydroxylation weight loss of 31.2% agrees with the calculated value of 31.0%.

Sample AR-24 (top curve in Fig. 3) comprised hydrotalcite plus minor unreacted MgO. Following Miyata (12) the two DTA peaks at 237 and 409°C were assigned to loss of interlayer water and loss of OH^- + CO_3^{2-} (as H_2O and CO_2), respectively. The observed TGA weight losses can be compared with values calculated from the aluminum removal reaction. The latter was established from the [Al]/[Al + Mg] ratio for hydrotalcite (derived from XRD determination of a) and the measured weight increase during aluminum removal (82.8% for AR-24). The reaction is

$$MgO + (Al, CO_3, H_2O) \rightarrow 0.46\,MgO + 0.71$$
$$[Mg_{0.76}Al_{0.24}(OH)_2(CO_3)_{0.12}(H_2O)_{0.64}].$$
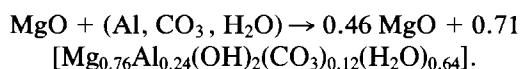
The calculated weight losses for the above product due to loss of interlayer water and OH^- + CO_3^{2-} are 11.1 and 24.3 wt%, re-

TABLE II

Al REMOVAL CONDITIONS AND THERMAL ANALYSIS RESULTS, AR-4, -24, AND -26

Run number	AR-4	AR-24	AR-26
$MgCO_3$ type	Laboratory grade $MgCO_3$	BDH basic carbonate	BDH basic carbonate
Calcination conditions	700°C, 1 hr	1100°C, 2 hr	1100°C, 2 hr
Initial [Al] (ppm)	100	1000	150
Soda strength (g liter^{-1})	260	260	260
Causticity	95	100	100
Solution temperature (°C)	80	80	80
Al removal time (hr)	1	1	1
Phases in precipitate (by XRD)	Brucite	Hydrotalcite (75%), MgO (25%)	1 : 1 intgrowth (67%), Brucite (15%), MgO (18%)
Precipitate wt% increase	44.5	82.8	57.0
Al removal (ppm)	25.2	173.0	78.9
DTA peak positions (°C)	95	90 (sh)	90 (sh)
	406	237	158
		409	370 (sh)
			406
TGA weight loss (%)	4.7 (<280°C)	14.1 (<280°C)	7.4, 7.7 (<280°C)
	31.2 (280–500°C)	23.5 (280–500°C)	22.3, 25.2 (>280°C)

spectively, compared with experimental TGA values of 14.1 and 23.5 wt%. The higher measured interlayer water loss of 14.1 wt% also includes some surface adsorbed water, as indicated by the low temperature tail in Fig. 3.

The DTA curve for the 1 : 1 intergrowth phase in AR-26 shows two endotherms at 158 and 406,370(sh)°C, the former having a tail extending to lower temperatures. By analogy with hydrotalcite, these were assigned to loss of interlayer water and loss of $OH^- + CO_3^{2-}$, respectively. The lower temperature of 158°C for interlayer water, cf 237°C for hydrotalcite, is consistent with the expanded interlayer spacing in the hydrotalcite part of the intergrowth phase, with an associated weaker attraction between the $M(OH)_2$ layers and the interlayer molecules. In contrast to brucite and hydrotalcite the higher temperature DTA peak for the intergrowth phase is split into two peaks, at 406 and 370°C. These presumably reflect the different binding strengths of the two independent hydroxyl ions associated with the brucite and hydrotalcite type interlayer regions.

The aluminum removal reaction for AR-26 is given below:

$$MgO + (Al, CO_3, H_2O) \rightarrow$$
$$0.29MgO + 0.16$$
$$Mg(OH)_2 + 0.62[Mg_{0.88}Al_{0.12}(OH)_2$$
$$(CO_3)_{0.06}(H_2O)_{0.32}].$$
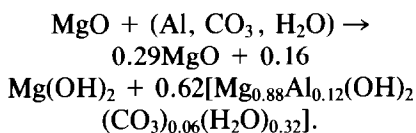
The calculated weight losses from interlayer water and $OH^- + CO_3^{2-}$ for this reaction are 5.6 and 25.7 wt%, respectively, which compare with the experimental values of 7.2, 7.4 and 22.3, 25.2 wt% for separate runs on AR-26.

4.3. Infrared Spectra

The infrared spectrum of the 1 : 1 intergrowth phase in AR-26 is compared with the spectra for hydrotalcite and brucite in Fig. 4. For brucite, a sharp $\nu(OH)$ at 3700 cm^{-1}, characteristic of $Mg(OH)_2$ (22), is the main feature. The broad peaks at 3440 and 1640 cm^{-1} are due to surface adsorbed water and the broad peak at 1470 cm^{-1} is due to CO_3^{2-}. This carbonate must also be present as a surface adsorbed species, since no carbonate compound was identified in the XRD pattern. The hydrotalcite sample shows a very broad $\nu(OH)$ band at 3530 cm^{-1} due to strongly H-bonded OH^- and H_2O, together with a shoulder at 3100 cm^{-1}. In the CO_3^{2-} region it exhibits a relatively sharp ν_3 peak at 1370 cm^{-1}. Both hydroxide and carbonate peak positions agree closely with reported values for synthetic hydrotalcite with [Mg]/[Al] = 3 (23).

The spectrum for the 1 : 1 intergrowth phase shows peaks that lie between those for hydrotalcite and brucite, consistent with its intermediate composition and structure. Thus $\nu(OH)$ peaks are at 3630 and 3440 cm^{-1} and $\nu(CO_3^{2-})$ is at 1400 cm^{-1}. Peaks are also present due to $Mg(OH)_2$ (3710 cm^{-1}) and surface adsorbed water.

4.4. Comparison with the Structure of Coalingite

During the preparation of this article we came across a reference to a magnesium iron hydroxycarbonate mineral coalingite,
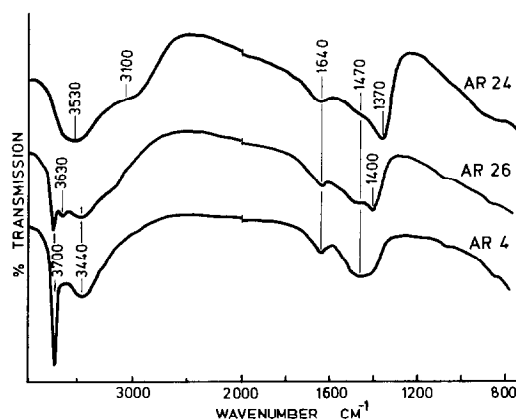
FIG. 4. Infrared spectra for AR-4, AR-24, and AR-26, containing predominantly brucite, hydrotalcite, and the 1 : 1 intergrowth phase, respectively.

which has the same XRD powder pattern as the 1:1 intergrowth phase (24). A single-crystal structure determination was reported for coalingite (25) which supports the structure we deduced for the intergrowth phase, shown schematically in Fig. 2. Coalingite is rhombohedral, $R\bar{3}m$, with $a = 3.12$ Å and $c = 37.4$ Å. Its composition is reported to be $Mg_{10}Fe_2(OH)_{24}(CO_3) \cdot 2H_2O$ (24). Expressed in terms of $M(OH)_2$ this gives $Mg_{0.833}Fe_{0.167}(OH)_2(CO_3)_{0.083}$ $(H_2O)_{0.167}$, which has an $[M^{3+}]/[M^{2+} + M^{3+}]$ ratio of 0.167, considerably higher than the value of 0.12 for the magnesium aluminum phase. The number of oxygens per interlayer sheet is 0.833, which is less than the value of 1.0 corresponding to close packing that we assumed in our formula but consistent with interlayer oxygen contents of less than 1.0 in hydrotalcites (26). The single-crystal studies showed broadening and streaking of reflections along lines parallel to c^*, and powder patterns gave poor fits between calculated and observed line positions, particularly for the basal plane reflections, as we observed for the 1:1 intergrowth phase. This was interpreted as due to irregularities in the stacking sequence of two $M(OH)_2$ layers and one carbonate–water layer.

5. Higher Order Intergrowths

The preliminary aluminum removal studies described above were followed up with a systematic study of aluminum removal from simulated white liquors as a function of solution and MgO-additive variables. The variables studied were type of magnesium carbonate and calcination temperature, soda strength, causticity and temperature of the white liquor, concentration of aluminum in solution, amount of added MgO, and reaction time. Over 300 experiments were performed, AR-1 to -308, the full results of which will be published elsewhere.

The most important parameter affecting aluminum removal was found to be the solution temperature. Results are given in Table III for experiments using calcined hydromagnesite in solutions for which the temperature was varied in the range 40 to 90°C. The composition of the precipitated phase was a sensitive function of solution temperature, with intergrowths containing higher brucite:hydrotalcite ratios forming with increasing temperature.

At the lowest solution temperature studied, 40°C, hydrotalcite was the dominant phase formed and complete removal of aluminum from solution was achieved. At 60°C, the amount of hydrotalcite had halved and the 1:1 intergrowth phase had begun to form. Despite a greater conversion of MgO to hydroxycarbonates at the higher temperature the amount of aluminum removed was lower. This is consistent with the lower incorporation of aluminum into the intergrowth phase relative to hydrotalcite. At 70°C the 1:1 intergrowth phase was the only hydroxycarbonate formed, together with minor brucite.

At 80°C a new intergrowth phase was observed, with the strongest basal reflections at $d = 5.8$ and 4.4 Å. Both the positions and intensities of the XRD peaks are in accord with a 2:1 brucite:hydrotalcite intergrowth with $c' = 17.5$ Å. A magnesium iron hydroxycarbonate mineral, coalingite-K, has been reported which has the same XRD powder pattern (24) as the 2:1 intergrowth phase. At 90°C the intergrowth peaks were very broad and weak, corresponding to a range of higher order intergrowths, with the main component a 4:1 intergrowth. The dominant hydroxide product in this case was brucite and the aluminum removal was only 44%.

When the soda strength was increased to 500 g liter^{-1}, run AR-83 in Table III, the XRD pattern for the precipitated product showed brucite and residual MgO as the only phases. However, despite the absence

TABLE III

RESULTS OF ALUMINUM REMOVAL EXPERIMENTS

| | Mg-additive | | White liquor conditions | | | | Reaction time | Phases in precipitated product (heights of XRD peaks (cps))[a] | | | | Al removed | |
Run No.	Type	Calcination temperature	Soda strength	Causticity	Solution temperature	[Al] (ppm)	(hr)	Brucite	Intergrowth	Hydrotalcite	MgO	(ppm)	Comments
XRD peak heights of pure phases								17,000	2,500	21,000	40,000		
AR-195	HM	1,000	260	95	40	100	1	1,100	—	5,300	5,000	100	HM, hydromagnesite
AR-187	HM	1,000	260	95	60	100	1	2,400	300	2,800	400	78.6	
AR-179	HM	1,000	260	95	70	100	1	2,600	600	—	—	65.2	Intergrowth = 1 : 1
AR-183	HM	1,000	260	95	80	100	1	4,100	200	—	—	60.4	Intergrowth = 2 : 1
AR-175	HM	1,000	260	95	90	100	1	6,500	200	—	—	43.8	Intergrowth ~4 : 1
AR-83	BDH	1,150	500	100	80	150	1	15,300	—	—	6,100	47.0	LR grade $MgCO_3$
AR-10	BDH	1,100	260	"100"	80	100	1	1,500	900	—	10,700	45.0	Causticity nominally
AR-20	BDH	1,100	260	"100"	80	100	2	2,200	700	—	4,500	59.5	100%. Some CO_2
AR-21	BDH	1,100	260	"100"	80	100	4	4,000	300	—	1,500	61.5	from atmosphere.

[a] Peak intensities (cps) for brucite, 1 : 1 intergrowth, hydrotalcite, and MgO at d = 4.8, 6.4, 7.8, and 2.11 Å, respectively.

of mixed metal hydroxycarbonates, 47 ppm of the original 150 ppm of aluminum was removed. This seemingly paradoxical result is due to the incorporation of aluminum into the brucite structure. This was confirmed by a refinement of the unit cell parameters, giving $a = 3.133(1)$ Å and $c = 4.746(5)$ Å. Using the linear a vs [Al]/[Al + Mg] relationship for aluminum-containing brucites (17) gives an atomic fraction of aluminum of 0.025 in the $M(OH)_2$ layers. Charge balance is presumably maintained by incorporation of interlayer OH^- and/or CO_3^{2-}, although at such a low level of aluminum there is no long-range cooperative ordering of the brucite and hydrotalcite-like segments. Thus aluminum-containing brucites are disordered, brucite-rich, higher order intergrowth phases.

From time-series experiments, runs 10, 20, and 21 in Table III, we obtained evidence that the ordered intergrowth phases are metastable and eventually transform to aluminum-containing brucite. For the conditions described in Table III the 1 : 1 intergrowth phase became unstable relative to brucite after 2 hr, when the aluminum concentration in solution had dropped below 40 ppm. Measurement of the XRD peak positions for brucite in the product from run AR-21 gave an a parameter of 3.125 Å, corresponding to a relatively high atomic fraction of incorporated aluminum, 0.04 (17). A conversion of hydrotalcite to the 1 : 1 intergrowth phase was observed in a similar series of experiments using higher aluminum concentrations. The destabilization of hydrotalcite relative to 1 : 1 intergrowth occurred when [Al] in solution fell below 130 ppm.

Acknowledgments

References

1. H. HOLTON, Pulp Pap. Can. 78, T218 (1977).
2. A. J. BENNETT, J. D. GILLETT, AND H. WUNDER, Appita 35, 383 (1982).
3. P. ULMGREN, Nord. Pulp Pap. Res. J. 2, 4 (1987).
4. N. S. KURNAKOV AND V. V. CHERNYKH, Zap. Ross. Mineral. Ova. 55, 118 (1926).
5. C. FRONDEL, Am. Mineral. 26, 295 (1941).
6. R. ALLMANN AND H. LOHSE, Neues Jahrb. Mineral. Monatsh. 6, 161 (1966).
7. R. ALLMANN, Acta Crystallogr. 24, 972 (1968).
8. W. FEITKNECHT AND M. GERBER, Helv. Chim. Acta. 25, 131 (1942).
9. M. M. MORTLAND AND M. C. GASTUCHE, C.R. Acad. Sci. 255, 2131 (1962).
10. M. C. GASTUCHE, G. BROWN, AND M. M. MORTLAND, Clay Miner. 7, 177 (1967).
11. S. MIYATA, Clays Clay Miner. 23, 369 (1975).
12. S. MIYATA, Clays Clay Miner. 28, 50 (1980).
13. H. BESSON, S. CAILLERE, AND S. HENIN, Bull. Groupe Fr. Argiles 26, 79 (1974).
14. H. BESSON, S. CAILLERE, AND S. HENIN, Clay Miner. 12, 239 (1977).
15. R. ALLMANN, Fortschr. Mineral. 48, 24 (1971).
16. I. PAUSCH, H.-H. LOHSE, K. SCHURMANN, AND R. ALLMANN, Clays Clay Miner. 34, 507 (1986).
17. G. MASCOLO, O. MARINO, AND A. CANTARELLI, Trans. J. Br. Ceram. Soc. 79, 6 (1980).
18. J. H. CANTERFORD, P. T. L. KOH, C. MOORREES, AND G. TSAMBOURAKIS, Bull. Proc. Australas. Inst. Min. Metall. 290, 71 (1985).
19. A. J. BENNETT, H. WUNDER, AND J. SCUKOVIC, Appita 40, 265 (1987).
20. G. W. BRINDLEY AND S. KIKKAWA, Am. Mineral. 64, 836 (1979).
21. G. MASCOLO AND O. MARINO, Mineral. Mag. 46, 136 (1982).
22. R. K. VANDERLAAN, J. L. WHITE, AND S. L. HEM, J. Pharm. Sci. 71, 780 (1982).
23. M. J. HERNANDEZ-MORENO, M. A. ULIBARRI, J. L. RENDON, AND C. J. SERNA, Phys. Chem. Miner. 12, 34 (1986).
24. F. A. MUMPTON, H. W. JAFFE, AND C. S. THOMPSON, Am. Mineral. 50, 1893 (1965).
25. J. PASTOR-RODRIGUEZ AND H. F. W. TAYLOR, Mineral Mag. 38, 286 (1971).
26. H. F. W. TAYLOR, Mineral. Mag. 39, 377 (1973).